2009-k-41

Semi-automatic Recognition of Lunar Geologic Units Based on Texture and Spectral Features Using Image Data Observed by Kaguya TC/MI

By Yuto SHIBATA[1], Noriaki ASADA[1], Naru HIRATA[1], Hirohide DEMURA[1], Yasuhiro YOKOTA[2], Tomokatsu MOROTA[2], Chikatoshi HONDA[2], Tsuneo MATSUNAGA[3], Makiko OHTAKE[2], Junichi HARUYAMA[2]

[1]*The University of Aizu, Japan,* [2]*JAXA, Japan*
[3]*National Institute for Environmental Studies, Japan*

This paper demonstrates experimental procedures for semi-automatic recognition of lunar geologic units based on the photogeological characteristics such as texture and spectral features on images. Multi-spectral image data observed by Multi-band Imager (MI) onboard KAGUYA are used as test data. Digital number of variance in certain area is extracted as a texture feature, and two kinds of image calculation, band ratio are extracted as spectral features. And then, each pixel is classified in some classes based on these two features. The result of classification shows capability of recognition method proposed in this work.

Key Words: Kaguya (SELENE), Geological map, Texture, Spectrum, Classification

1. Introduction

Recognition of geologic units on image data is a fundamental analytical step of remote sensing. A single geologic unit could be defined as a region with its own particular features on the image, which represent its origin. The same units have common photogeological characteristics such as texture and spectral features. Criteria for determining the units are varied between previous and recent researches. In 1960’s and 1970’s, researchers in lunar science used panchromatic photographs to make lunar geologic maps. Their basic criteria of geologic units are defined by surface textures and topographic features in the photographs. Recently, variation of remote sensing data has greatly expanded. Resolution and coverage of image data are increase, and multi-spectral images of the moon have been obtained through modern lunar missions[1]. We especially focus on recognition of geologic units by combining both texture and spectral features extracted from image data.

In addition, many techniques for automatic or semi-automatic image classification are developed[2,3]. If these techniques are effective for recognition of geologic units in remote sensing data, automatic or semi-automatic data processing would be an important method for production of geologic maps of the moon. The author tries to consider the capability of these image classification techniques with lunar high-resolution images and multi-spectral images obtained by Terrain Camera[4] (TC) and Multiband Imager[5] (MI) onboard the Kaguya lunar explorer.

Texture is a small-scale pattern on images. It is a reflection of surface undulation and reflectance of the object, and affected by lighting conditions. While the surface undulation controls the texture at low solar elevations, the reflectance governs at high solar elevations. The variance of digital number of pixels in certain area is a one of the statistical indices for textual features, and is adopted in this research. Spectral features are representation of characteristics of reflectance spectra of materials. They are derived from image calculations of multi-spectral image data. Band ratio is one of the simplest and widely utilized spectral features[6]. The band ratios are indicator of the slope of spectral continuum or the depth of absorption bands. For the lunar case, they represent the contents of mafic minerals and the degree of space weathering[7]. Previous researchers mentioned nothing about combining the texture and spectral features for automatic lunar geological mapping.

K-means clustering algorithm is adopted to label pixels based on the texture and spectral features in this research. The algorithm is one of the most popular methods for unsupervised image classification. Unsupervised classification is an automated process for finding cluasters of data

The purpose of this research is to create a vision for automatic or semi-automatic geological mapping based on some photogeological characteristics such as texture and spectrum on image. In this paper, for achieving automatic geological mapping, semi-automatic recognition of geological units were shown by following three steps; 1) Extraction of texture and spectral features, 2) Classification by k-means method based on both two features, 3) Evaluation of the results of classification.

2. Method

An experimental procedure for semi-automatic recognition of geologic units proposed in this paper is shown on Fig. 1. There are four consecutive steps in this procedure.

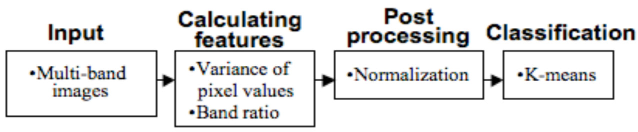

Fig. 1. An experimental procedure in this work

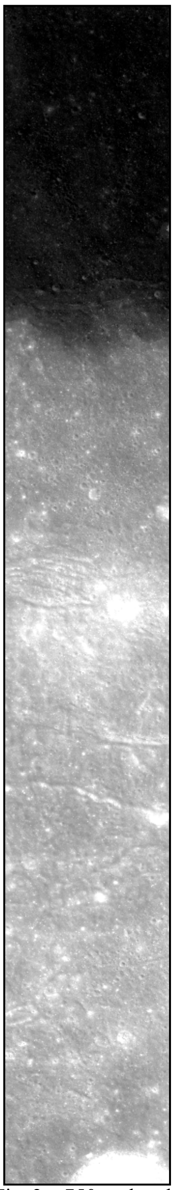

Fig. 2 750nm band image

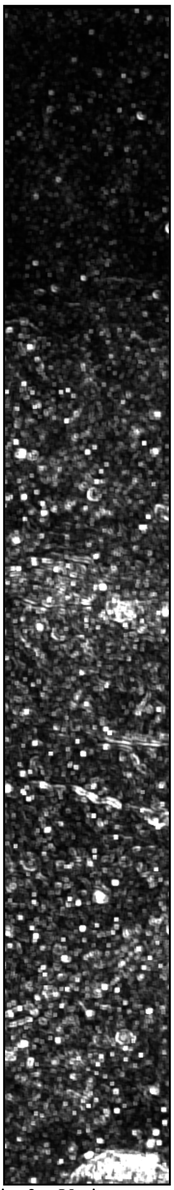

Fig. 3 Variance map (Texture feature)

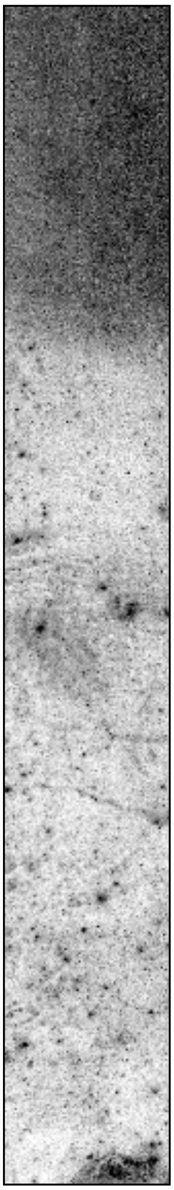

Fig. 4(a) 750/415nm (Spectral feature)

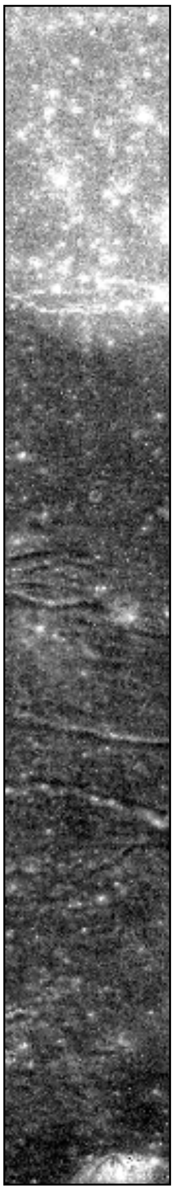

Fig. 4(b) 750/950nm (Spectral feature)

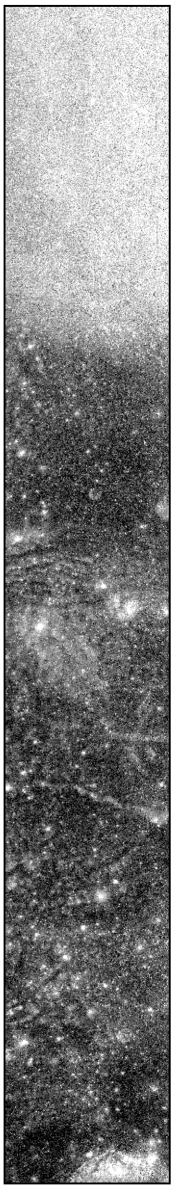

Fig. 4(c) 415/750nm (Spectral feature)

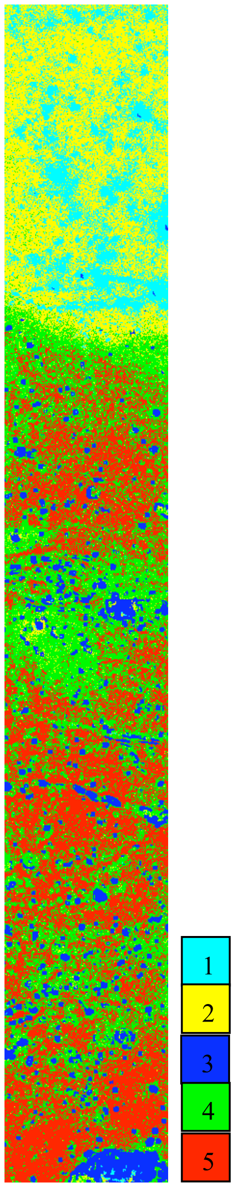

Fig. 5 K-means classification map

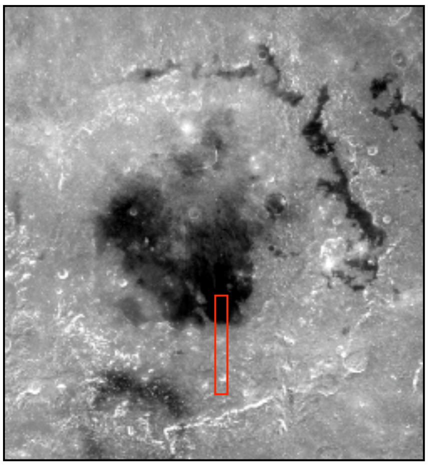

Fig. 6 Orientale basin taken by the Lunar Orbiter. The red rectangle corresponds to the area of test data (Fig. 2).

2.1 Giving the Variance of Pixel Values as Texture Features

The value of variance is acquired by a filtering process with a square-shaped filter. The size of the square filter is 21 x 21. This filter size corresponds to about 420 x 420 m in real scale. The variance in this research is as follows;

$$Variance = \sum_{l=0}^{l\,\max} (l - Mean)^2 P(l)$$

where *l* means a pixel values and *P(l)*, l = 0, 1, 2, ... ,*lmax* , is frequency of each l.

2.2 Giving the Ratio Images as Spectral Features

Three combinations of the MI band are adopted to take the band ratios; 750nm/415nm, 750nm/950nm, and 415nm/750nm. They are common sets for lunar multi-band images.

2.3 Normalization

The value of variance and band ratio are normalized to the interval [0, 1] because the difference in the dynamic range in the two features affects clustering results as weighting.

2.4 Classification by K-means Clustering

K-means clustering method is used for classification based on the three factors: variance, 750/415nm, and 750/950nm. Because 415/750nm is a reciprocal number of 750/415nm, one of them is selected. The number of classes is set at 5. Each class is colored by the result of classification for visualization.

3. Used Data

Nine-bands multi-spectral images observed by the Multi-band Imager (MI) are used as test data of the classification procedure proposed in this paper. The MI observed the lunar surface at VIS (415nm, 750nm, 900nm, 950nm, 1000nm) and NIR (1000nm, 1050nm, 1250nm, 1550nm) in wavelength. The author remarked only three bands 415nm, 750nm, and 950nm in nine bands because of the spectral features mentioned in this introduction. The resolution of 3 images are 20m/pixel. Fig. 2 is single band image (750nm) observed by MI. This image shows the southern central area of the Orientale basin at 93°W, 24°S, and the image coverage is 20 x 122 km. We find a part of large basaltic deposits and highland in Orientale basin with many pristine impact craters.

4. Results

Fig. 3 shows a result of the filtering process for extracting variance from single band image of MI (750nm). Bright pixels in Fig. 3 represent large variance regions and dark ones are small variance regions. Figs. 4(a)-(c) show the results of band ratio, 750/415nm, 750/950nm, and 415/750nm, respectively. The bright pixels in Fig. 4 show large ratio region and dark ones show small ratio region. Fig. 5 shows a result of k-means clustering based on the variance map and the band ratio maps of 750/415nm, and 750/950nm. The number of class is 5, and each class is colored with different color.

5. Discussion

5.1 Variance Data

Figs .7 show close-up views of original 750nm image (Fig. 2) and variance map (Fig. 3). Fig. 7(a) and (b) show at the same area each other. Fig. 7(a) is a part of basaltic area, and there are little pristine on original 750nm image. Therefore the area in Fig. 7(b) shows almost small variance pixels (dark). Fig. 7(c) and (d) also show at the same area each other. Distribution of large variance pixels (white) shows spotty squared patterns in the Fig. 7(d). It corresponds to pristine craters on the original 750nm image (Fig. 7(c)).

5.2 Ratio images

Figs. 8 show close-up views of original 750nm image (Fig. 2) and band ratio maps (Figs. 4(a), (b)). Figs. 8(a), (b), and (c) show the same area each other. Upper dark area in Figs. 8(a) is basaltic deposit in Orientale basin. In contrast, lower bright area is composed of highland material. In Figs. 8(b), the value in the bottom highland shows larger than the top basaltic deposit. Therefore the bottom highland and top basaltic sediments are composed of variant materials, and they might be affected by space weathering. In Figs. 8(c), spotty pattern of large values are shown in the side of top basaltic area. In contrast, few spotty patterns are found in the bottom highland. Therefore the top basalt corresponds to the mafic-rich area.

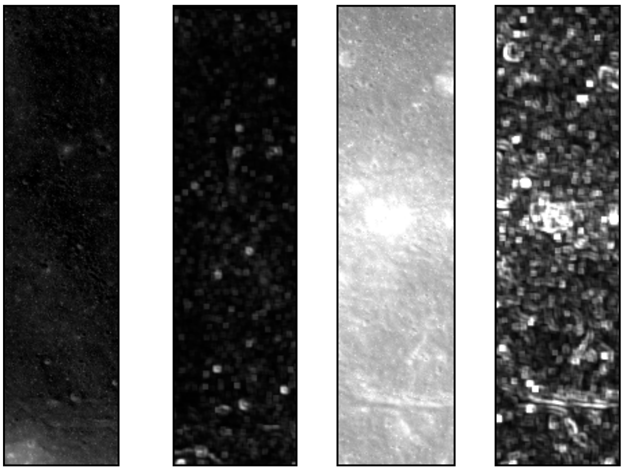

(a) (b) (c) (d)

Figs. 7 Close-up views of original 750nm image (a, c) and variance map (b, d). The area of (a) and (c) is the same one in (b) and (d).

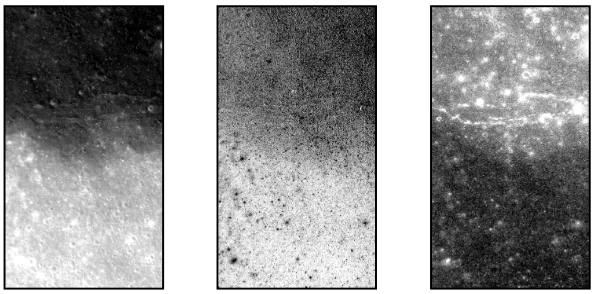

(a) (b) (c)

Figs. 8 Close-up views of original 750nm image (a) and band ratio maps, 750/415nm and 750/950nm (b, c).

5.3 Classification

Table 1 shows evaluation table of each 5 class. In this section, 5 classes and input features are compared each other, and characteristics of 5 classes are shown.

Table 1. Evaluation of the result of classification (k=5)

class	Variance	750/415nm	750/950nm
1	Small	Small	Large
2	Small	Small	Middle
3	Large	Small	Large
4	Middle	Middle	Middle
5	Small	Large	Small

5.3.1 Class 1 and 2

Figs. 9 show close-up views focusing on class 1 (blue) and 2 (yellow). Figs. 9(a), (b), and (c) are variance, 750/415nm, and 750/950nm map, respectively. Figs. 9(d) is a classification result. The value of variance and 750/415nm in the class 1 and 2 is small. On the other hand, the value of 750/950nm in class 1 is larger than class 2. Therefore the factor dividing class 1 and 2 is the spectral feature, "750/950nm". Variance and 750/415nm could not be factors to divide class 1 and 2. Moreover the class 1 and 2 could be mafic-rich classes because larger value in 750/950nm corresponds to these two classes.

5.3.2 Class 3

Figs. 10 show close-up views focusing on class 3 (navy). The value of 750/950nm in the class 3 is as large as that in the class 1. The difference between class 3 and 1 results from the value of variance as the table 1 says. The class 3 matches the area of the larger variance area. If the area that class 3 and 1 show are different from the viewpoint of lunar geology, the usability of texture and spectral features for semi-automatic recognition of geologic units would be shown.

5.3.3 Class 4

Figs. 11 show close-up views focusing on class 4 (green). In the class 4, the value of all features, variance, 750/415nm, and 750/950nm is middle. Pixels on the periphery of boundary between upper basaltic and highland area in test data are classified into the class.

5.3.4 Class 5

Figs. 12 show close-up views focusing on class 5 (red). The class 5 corresponds to large value area in 750/415nm, and small value area in 750/950nm. Therefore, the area in class 5 corresponds to mafic poor area because of the value of 750/950nm. And it could be space-weathered area class because of the value of 750/415nm.

6. Summary and Future Works

This research showed the capability of semi-automatic recognition of geologic units with following procedures; 1) Extraction of the texture and spectral features from multi-spectral image data taken by Multiband Imager onboard KAGUYA, 2) Classification based on these two features, 3) Evaluation of the classification result for recognizing geological units.

The two kinds of features, variance as texture features and band ratio as spectral features are used on a trial basis in this work although more accurate recognition of geologic units may need more information as indicator of geological characteristics. In the field of image processing, calculation of the entropy, skewness and another statistical features has already proposed other than variance. In the recent lunar geological research, calculation for the contents of TiO_2, FeO and absorption band depth, which decide the material types on the lunar surface directly has been already proposed too. Texture and spectral features extracted from images have wide variety. For future works, we examine the combination of another texture and spectral features for raising the precision of semi-automatic recognition of lunar geologic units proposed in this work.

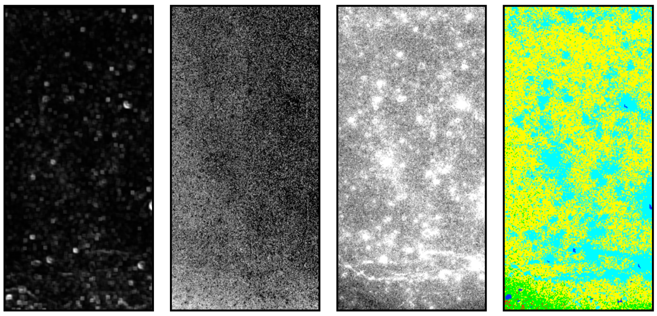
(a) (b) (c) (d)

Figs. 9 Close-up views focusing on class 1 (blue) and 2(yellow). (a), (b), and (c) are variance, 750/415nm, 750/950nm maps, respectively.

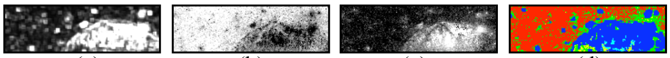
(a) (b) (c) (d)

Figs. 10 Close-up views focusing on class 3 (navy). (a), (b), and (c) are variance, 750/415nm, 750/950nm maps, respectively.

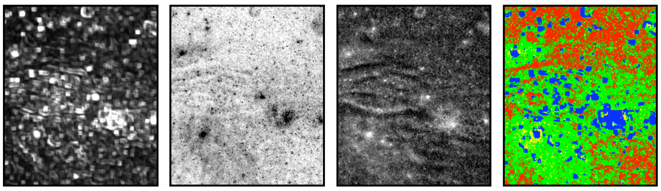
(a) (b) (c) (d)

Figs. 11 Close-up views focusing on class 4 (green). (a), (b), and (c) are variance, 750/415nm, 750/950nm maps, respectively.

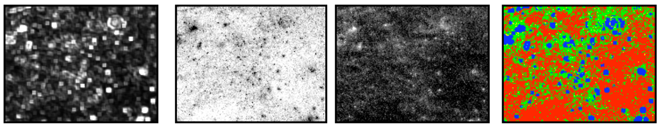
(a) (b) (c) (d)

Figs. 12 Close-up views focusing on class 5 (red). (a), (b), and (c) are variance, 750/415nm, 750/950nm maps, respectively.

Acknowledgments

We appreciate cooperation of the members of the Multimedia Systems Lab of the University of Aizu, especially in K. Kimura, who researched the effectiveness of texture features for making geological map and graduated from the University of Aizu on March, 2008.

References

1) Stewart Nozette, P. Rustan, L. P. Pleasance, D. M. Horan, P. Regeon, E. M. Shoemaker, et al: *The Clementine Mission to the Moon: Scientific Overview*, Science, **266** (1994), pp. 1835-1839
2) Refael C. Gonzalez, Richard E. Woods: *Digital Image Processing*, Prentice Hall Press, 2001, pp
3) W. G. REES: Physical Principles of Remote Sensing, Cambridge

University Press, 1990, pp.209-220

4) Junichi Haruyama, Tsuneo Matsunaga, Makiko Ohtake, Tomokatsu Morota, Chikatoshi Honda, Yasuhiro Yokota, Masaya Torii, Yoshiko Ogawa: *Global lunar-surface mapping experiment using the Lunar Imager/Spectrometer on SELENE*, Earth Planet Space, **60** (2008), pp.243-255
5) Makiko Ohtake, Junichi Haruyama, Tsuneo Matsunaga, Yasuhiro Yokota, Tomokatsu Morota, Chikatoshi Honda: *Performance and scientific objectives of the SELENE (KAGUYA) Multiband Imager*, Earth Planet Space, **60** (2008), pp.257-264
6) C. M. Pieters, M. I. Staid, E. M. Fischer, S. Tompkins, G. He: *A Sharper View of Impact Craters from Clementine Data*, Science, **266** (1994), pp. 1844-1847
7) C. M. Pieters, L. A. Taylor, S. K. Noble, L. P. Keller, B. Hapke, R. V. Morris, C. C. Allen, D. S. Mckay, S.Wentworth: *Space weathering on airless bodies: Resolving a mystery with lunar samples*, Meteoritics and Planetary Science **35** (2000), pp.1101-1107